



# Measurements of the radiation resistant fused quartz radioluminescence spectral intensity under irradiation in the pulse nuclear reactor

A. Gorshkov<sup>a</sup>, D. Orlinski<sup>a,\*</sup>, V. Sannikov<sup>a</sup>, K. Vukolov<sup>a</sup>, S. Goncharov<sup>b</sup>,  
Yu. Sadovnikov<sup>b</sup>, A. Kirillov<sup>b</sup>

<sup>a</sup> Russian Research Centre, Kurchatov Institute, Kurchatov Sq. 1, 123182 Moscow, Russian Federation

<sup>b</sup> CC Atomsafety, Sergiev Posad-7, Moscow Region 141300, Russian Federation

Received 11 November 1998; accepted 16 February 1999

## Abstract

The radioluminescence spectral intensity of KU-1 and KS-4V fused quartz under neutron and gamma pulse irradiation was measured in the visible range (380–700 nm) in the pulse nuclear reactor BARS. Three groups of quartz samples were tested during the experiments, the first group – nonirradiated, the second and the third – preirradiated in the conventional nuclear reactor IR-8 up to neutron fluences of  $6 \times 10^{19}$  n/cm<sup>2</sup> (total absorbed dose 2.8 GGy (Si)) and  $6 \times 10^{18}$  n/cm<sup>2</sup> (total dose 0.3 GGy). The measurements were performed at temperatures of 18°C and 100°C. The intensity was quantified in terms of the photon emission, and the comparison was done with an estimated bremsstrahlung intensity for ITER plasma parameters. It is shown that KU-1 fused quartz is suitable for use as windows in the visible spectral range for ITER diagnostics. © 1999 Elsevier Science B.V. All rights reserved.

## 1. Introduction

General problems for optical plasma diagnostics in future thermonuclear reactors are a transparency degradation and a radioluminescence of optical materials under neutron and gamma irradiations. The transparency degradation of windows and lenses leads to losses of the measured light intensity, and the luminescence increases the background emission. To understand the influence of these factors on optical qualities of different glasses their investigation must be done in conditions as near as possible to those of fusion reactors.

As it is known from previous publications [1] fused quartz has a higher radiation resistance for the induced absorption and a much lower luminescence intensity compared to other silica glasses and sapphire. It is very important to know about both of these characteristics

for the correct choice of the location of windows and lenses in diagnostic channels inside the shield. Up to now the induced absorption was observed under different kinds of irradiation (see for instance Ref. [2]), but a radioluminescence of the quartz samples was registered only under gamma and electron irradiation [3] or in the more complicated fiberoptic systems. Measurements in the nuclear reactor were done only in arbitrary units [4]. Recently the KU-1 luminescence was measured under electron (2 MeV accelerator) [5], gamma (<sup>60</sup>Co-source) and neutron (DT-neutron generator) [6,7] irradiations.

The luminescence of small size KU-1 samples in constant neutron and gamma fluxes will only be observed if they are located in one of the nuclear reactor central channels in a very intense neutron flux. Another possibility consists in taking advantage of the pulse nuclear reactor: (1) very high power in a short pulse during which the sample transparency does not change appreciably and (2) it is not necessary to put the sample in a reactor channel, but to locate it outside the reactor core near to the lateral wall. The absolute measurements of the radioluminescence spectral intensity in the

\* Corresponding author. Tel.: +7-095 196 7587; fax: +7-095 943 0073; e-mail: orlinsk@qq.nfi.kiae.su

wavelength region of 380–700 nm presented here have been done in the pulse nuclear reactor BARS. Initial measurements were done in the spectral region of 450–700 nm and after system modifications in the region of 380–500 nm.

## 2. Experiment description

The general experiment layout is shown in Fig. 1. The tested samples of KU-1 quartz (impurities, in ppm, are Al –0.4, Ca –1.0, Fe –1.6, Ti –0.01, K –1.7 and OH –820) are mounted in a fixed position at a distance of about 10 cm from the reactor core surface. The radioluminescence is passed out from the reactor hall by the relay optics including three flat mirrors and is focused by a lens on the entrance slit of the spectrometer. All photodetectors and the data acquisition system are located in a neutron shielded room.

The radioluminescence spectrum is analyzed by the grating spectrometer. The 10-channel spectrometer has a 300 grooves/mm grating, a  $f/10$  relative aperture and a 27.5 nm/channel dispersion. The luminescence is trans-

mitted by a 10-channel light guide collector to the inputs of photomultipliers (photocathode of S-20 type). To protect this equipment against secondary gamma-radiation a lead shield was used. The used spectral range (450–700 nm) was limited by the transmission of the plastic fibers for short wavelengths and by the photomultiplier sensitivity for long wavelengths.

The operation of the equipment is synchronized with the reactor pulse. The signals from the photomultiplier block enter the ADC (the sampling step of 1.6  $\mu$ s) in the CAMAC crate. The neutron and gamma fluxes were monitored in the sample position during each pulse.

For absolute calibration of the measuring system the standard band lamp was used with the tungsten tape and with the known photon emission efficiency spectral distribution per unit solid angle  $S_{\text{stand}}(\lambda)$ . A standard lamp was placed instead of the sample. The geometry of the optical line and the registration efficiency were completely retained. Projection sizes of both the sample and the tungsten tape on the spectrometer entrance slit were less than the slit sizes. The radioluminescence of the total sample volume and the radiation of the total standard tape surface were measured. The comparison of the results allows to define the absolute radioluminescence intensity per unite sample volume. The radioluminescence photon emission efficiency  $S_{\text{RL}}(\lambda)$  was found as

$$S_{\text{RL}}(\lambda) = \frac{I_{\text{RL}} S_{\text{stand}}(\lambda) a_{\text{tape}}}{I_{\text{stand}} V_{\text{sample}}} [\text{Photons/cm}^3 \text{ nm sr}],$$

where  $I_{\text{RL}}$  and  $I_{\text{stand}}$  are the measured intensities of the radioluminescence and the standard lamp resp.,  $a_{\text{tape}}$  is the lamp tape surface area, and  $V_{\text{sample}}$  is the sample volume.

Three groups of quartz samples were tested during the experiment: the first group – nonirradiated; the other two were preliminary irradiated in the nuclear water-pool reactor IR-8 at the temperature 55°C. The second group was irradiated up to a neutron fluence of  $6 \times 10^{19}$  n/cm<sup>2</sup> ( $E > 0.1$  MeV) and gamma-dose 2.5 GGy (Si) (total absorbed dose: 2.8 GGy) and the third group – up to  $6 \times 10^{18}$  n/cm<sup>2</sup> ( $E > 0.1$  MeV) and gamma-dose 0.27 GGy (Si) (total absorbed dose: 0.3 GGy). The comparison of irradiated samples from the second and the third groups [8] has shown that all tested samples from the second group had a little bit higher transparency than the similar samples from the third group that may be explained as some kind of annealing at high gamma doses during irradiation. Typical optical density spectral distributions of unirradiated and irradiated KU-1 samples are shown in Fig. 2.

**Experimental conditions:** The neutron flux in the sample position reaches the maximum value of about  $10^{17}$  cm<sup>-2</sup> s<sup>-1</sup> during the pulse and together with gamma emission results in an absorbed dose rate up to  $3.6 \times 10^5$  Gy/s (Si). Neutron fluence per pulse  $6.5 \times 10^{12}$  n/cm<sup>2</sup>, gamma dose per pulse  $5.3 \times 10^{12}$  quanta/cm<sup>2</sup>, neutron

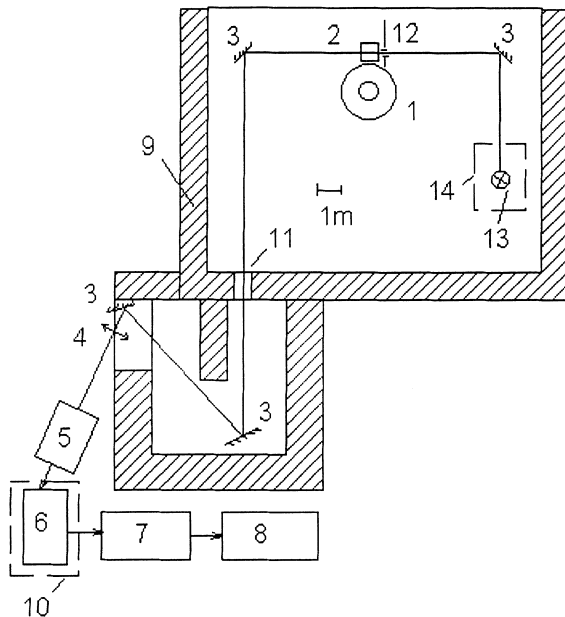


Fig. 1. General layout of the experiment: 1 – pulse nuclear reactor BARS; 2 – fused quartz sample; 3 – Al-coated mirrors, 4 – lens; 5 – spectrometer; 6 – box with ten photomultipliers; 7 – CAMAC ADC, 8 – personal computer; 9 – neutron shield from special concrete; 10 – lead shield; 11 – outlet in the shield ( $15 \times 15$  cm<sup>2</sup>); 12 – dark screen with a small hole; 13 – probing light source for the sample transparency check during the neutron pulse; 14 – standard light source shield from the neutron and gamma radiation.

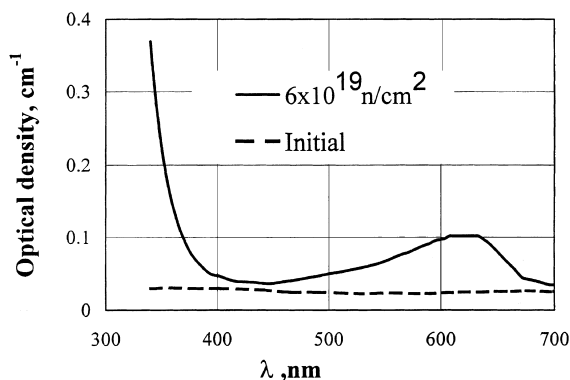


Fig. 2. Optical density of irradiated and nonirradiated quartz samples.

pulse duration (FWHM)  $\approx 60 \mu\text{s}$ , maximum neutron flux  $\approx 10^{17} \text{ n/cm}^2 \text{ s}$ , average neutron flux during the total pulse time ( $150 \mu\text{s}$ )  $4.3 \times 10^{16} \text{ n/cm}^2 \text{ s}$ , average gamma flux  $3.5 \times 10^{16} \text{ quanta/cm}^2 \text{ s}$ , average total absorbed dose rate during the total pulse time  $155 \text{ kGy/s}$  (Si), collecting solid angle  $2.9 \times 10^{-5} \text{ sr}$ , the sample diameter  $1.6 \text{ cm}$  and the sample thickness also  $1.6 \text{ cm}$ . Measurements were performed at sample temperature of  $18^\circ\text{C}$  and  $100^\circ\text{C}$ .

### 3. Results

Measurements of the radioluminescence spectral intensity were carried out in a visible range simultaneously for 10 spectral ranges. As an example, Fig. 3(a) presents the signals obtained from the neutron monitor and from two radioluminescence channels ( $\lambda = 530 \text{ nm}$  and  $\lambda = 667 \text{ nm}$ ) for the preliminary irradiated sample from the third group and a sample temperature of  $100^\circ\text{C}$ . One can see that this signal correlates well with the neutron pulse and there is no phosphorescence at the sensitivity level of the measurement system. The secondary  $\gamma$ -flux influence on the photomultiplier is small and only background pulses after the neutron pulse are induced. The signal pulse character has allowed one to construct the radioluminescence intensity dependence on the absorbed dose rate (Fig. 4). The linear dependence between these parameters is clear. Therefore, signal averaging over time is possible to increase the measurement accuracy. For the measurement results, signals were averaged over the whole neutron pulse time of  $150 \mu\text{s}$ . The luminescence intensity per unit sample volume, per unit spectral interval, and per unit solid angle, for an average absorbed dose rate of  $155 \text{ kGy/s}$  is given in Fig. 5. As one can see from the figure the preirradiated samples in comparison with nonirradiated samples have almost the same intensity from  $450$  to  $600 \text{ nm}$  and a little higher luminescence intensity (about 2–3 times) only at

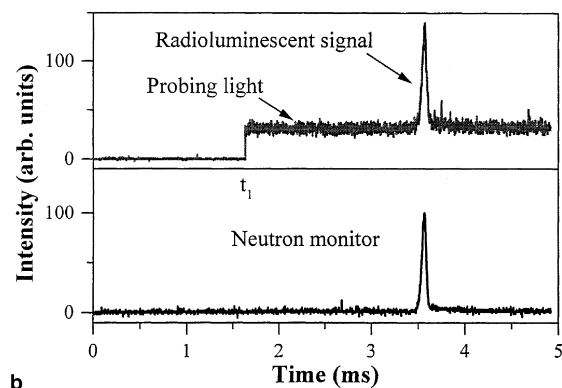
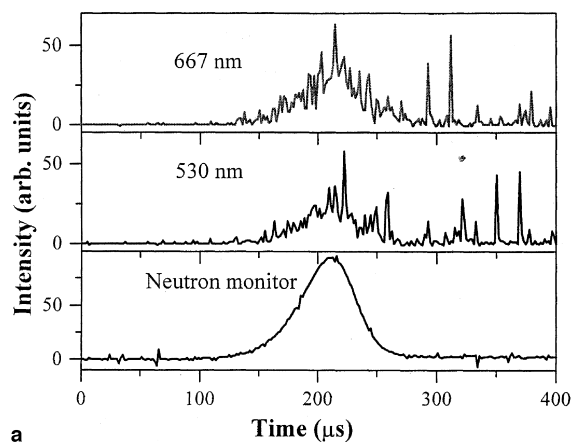


Fig. 3. Experimental signals: (a) radioluminescence intensity at  $\lambda \approx 530 \text{ nm}$  and  $\lambda \approx 667 \text{ nm}$  (for  $\Delta\lambda = 27.5 \text{ nm}$ ) and the neutron pulse; (b) neutron pulse and crown glass radioluminescence intensity together with the long probing pulse of the transparent light from an external source.

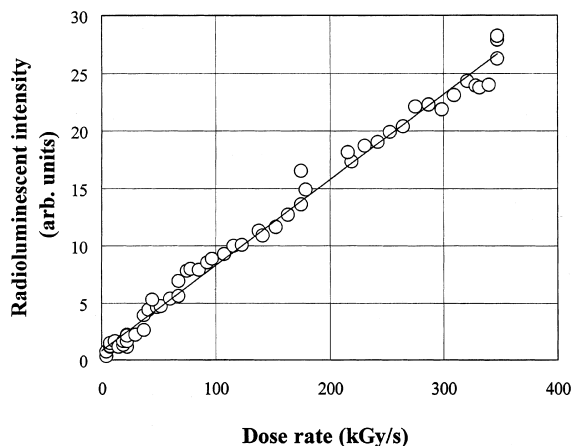


Fig. 4. The dependence of luminescence intensity on dose rate during one neutron pulse.

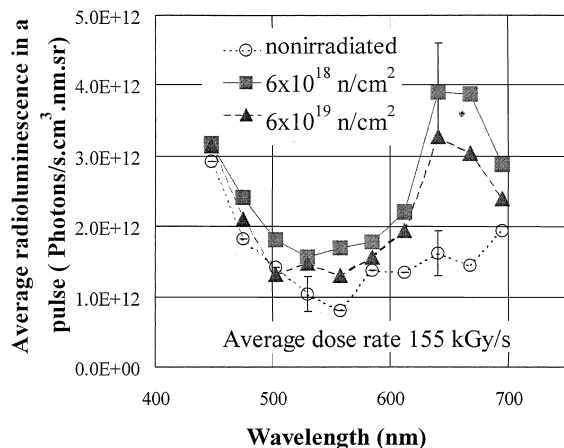


Fig. 5. Radioluminescence intensity spectral distribution for samples preirradiated in the stationary nuclear reactor.

wavelengths above 600 nm where the small difference for different irradiation doses corresponds to the difference in the induced optical density.

Previous measurements of the quartz KU-1 transparency dependence on the absorbed dose after [1] and during (in situ [9]) neutron and gamma irradiation have shown that in the spectral region of  $\lambda > 400$  nm the transparency almost does not change up to the neutron fluence of  $6 \times 10^{19}$  n/cm<sup>2</sup> and gamma dose of 2.8 GGy (with exception of a decrease by 10–15% at  $\lambda \approx 620$  nm). The above indicated data on neutron fluence and gamma dose per one reactor pulse ( $\approx 1$  Gy) are too small to influence the prompt transparency decrease. Nevertheless an additional check for the possible influence of the prompt absorption during the neutron pulse on the sample was carried out. For the test a sample crown glass was chosen also, which is much more sensitive to irradiation. The luminescence intensity and the intensity of the transparent light from the separate source (13 in Fig. 1) were measured simultaneously before, during and directly after the neutron pulse. The oscillograms in Fig. 3(b) shows that just after the luminescence pulse the transparent light intensity does not change; this means that the optical density of the sample does not change.

Measurements of the luminescence spectral intensity at different temperatures gave practically the same results for 18°C and 100°C (Fig. 6).

#### 4. KS 4V Quartz glass

Earlier a material comparison of different fiberoptics has shown that the best material for the core is the fused quartz KS-4V [10] which has an extremely low OH content (<0.2 ppm). Recent fiberoptic luminescence

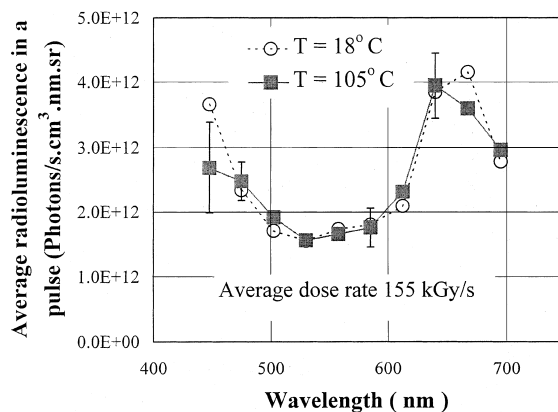


Fig. 6. Radioluminescence intensity spectral distribution for the samples at temperatures of 18°C and 100°C during irradiation.

measurements were made using the D–T neutron irradiation at TFTR [11] and an irradiation in the stationary reactor IR-8 [12]. In both cases some combined effects of induced absorption and radioluminescence were observed and in both cases the luminescence intensity was rather high. Therefore it is interesting to compare the luminescence intensity of irradiated core material KS-4V with known data for the KU-1 quartz. Radioluminescence spectral distributions for both glasses are given in Fig. 7. They are very similar. The difference in the short wavelength region is not important for the fusion reactor because neutron flux and gamma dose rate in the window regions will be much lower than in the present experiment, and a luminescence of both materials will not prevent from the measurement. These data support the supposition about the connection of the increased fiber-optic luminescence intensity with its complex structure.

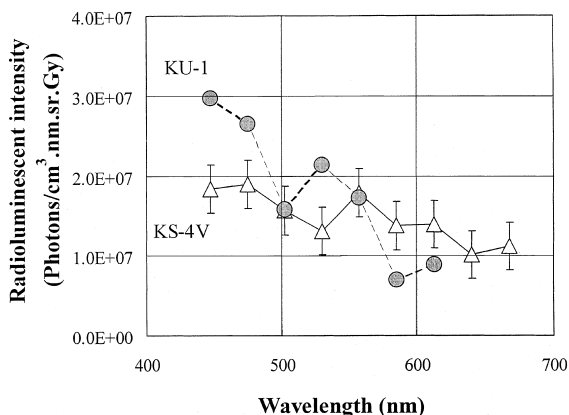


Fig. 7. Spectral distribution of the luminescence intensity of two quartz glasses under neutron and gamma irradiation in the pulse nuclear reactor.

## 5. Radioluminescence in the short wavelength region

The measuring system was modified to measure the radioluminescence intensity in a region of shorter wavelengths ( $\lambda = 380\text{--}500\text{ nm}$ ). (1) One flat mirror was added to the relay optic, (2) the lens before the spectrometer entrance slit was replaced by a spherical mirror, (3) the plastic fiber was replaced by a quartz fibre and (4) the tested KU-1 sample was replaced by another one with a size of 7 cm in diameter and 1 cm in thickness (volume increase more than one order of magnitude). All other parts of the system were the same as before. A rather small signal-to-background ratio in the near UV region did not allow enough accuracy. An attempt to extend the measuring range below 400 nm was not very successful, however additional results indicate no significant increase of the radioluminescence intensity in this region (Fig. 8).

## 6. Discussion

It is necessary to note that the luminescence measurements were done in the wavelength region in which the optical density of the KU-1 sample does nearly not depend on the irradiation dose. The strongest absorption bands are located at  $\lambda = 215$  and 260 nm. Beside these bands there are two low intensity bands at  $\lambda = 310$  and 620 nm. In the 620 nm region, the KU-1 transparency of 1 cm in thickness is decreased by  $\approx 15\%$  for an absorbed dose of  $\approx 2.8\text{ GGy}$ . A dependence of the radioluminescence intensity on the preirradiation is observed only in this spectral region (Figs. 2 and 5).

The registered level of the radioluminescence intensity is not higher than  $10^{-11}\text{ W s/cm}^3\text{ nm sr Gy}$  ( $3.5 \times 10^7$

photons/cm<sup>3</sup> nm sr Gy) inside the measured spectral range. This corresponds to the relative efficiency of the absorbed energy conversion into luminescent radiation energy in the indicated spectral region of about  $10^{-5}$  near to the value given in Ref. [1].

Results of the KU-1 quartz radioluminescence study as a function of the dose rate have shown that the luminescence intensity for the observed spectral range is proportional to the dose rate up to  $3.6 \times 10^5\text{ Gy/s}$  (Fig. 4). Thus it is possible to make a linear extrapolation of the measured intensity dependence on the dose rate for KU-1 quartz toward lower values. The neutron flux and the gamma dose rate calculated at the end of the optical periscopic (“dogleg”) diagnostic channel in the shielding block in ITER [13] will be lower by more than two orders of magnitude less than the neutron flux and the gamma dose rate in this experiment. To define the luminescence influence on the optical measurements the intensity of the bremsstrahlung from the plasma in the ITER ignition regime was estimated using the equation for the bremsstrahlung from Ref. [14] and the parameters of a plasma in the ignition regime from Ref. [13]. The bremsstrahlung intensity in this case will be not less than  $2 \times 10^{-6}\text{ W/cm}^2\text{ nm sr}$  ( $4.5 \times 10^{12}$  photons/cm<sup>2</sup> nm sr) in a visible range of the spectrum. The same luminescence intensity appears under BARS conditions for the quartz sample but at a neutron flux which is of 2–6 order of magnitude higher. Therefore under ITER conditions, the influence of the radioluminescence will be negligibly small for the quartz KU-1 window with several centimeters thickness.

Another important aspect of the radioluminescence of KU-1 quartz is the fact that there is almost no difference between preirradiated and nonirradiated samples. This means that even in a final phase of ITER operation the problem of the quartz optics luminescence can be neglected in the visible range.

## 7. Conclusions

1. Absolute values of the radioluminescence spectral intensity  $I_{RL}$  for KU-1 and KS-4V fused quartz samples due to gamma and neutron fluxes were obtained in the visible spectral range in respect of the gamma dose rate and the neutron flux close to the same conditions expected in ITER. The level of the luminescence intensity is less than  $10^{-11}\text{ W s/cm}^3\text{ nm sr Gy}$  ( $3.5 \times 10^7$  photons/cm<sup>3</sup> nm sr Gy) within the limits of the used spectral range of  $\lambda = 380\text{--}700\text{ nm}$ .
2. A dependence of  $I_{RL}$  on the dose rate is linear within the limits of the investigated spectral range up to 360 kGy/s.
3. In the visible spectral region the radioluminescence intensity  $I_{RL}$  of samples preirradiated up to a fluence

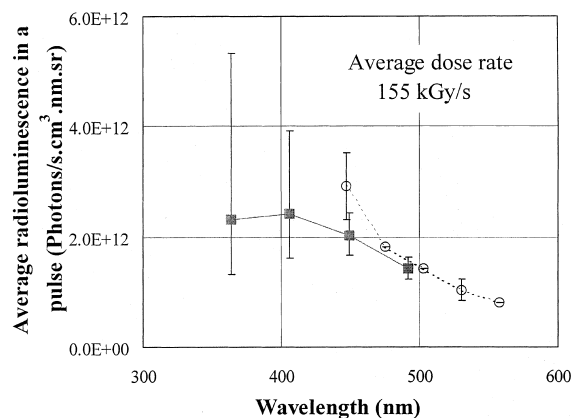


Fig. 8. Distribution of the quartz KU-1 radioluminescence intensity in the spectral region of 380–550 nm.

- of  $6 \times 10^{19}$  n/cm<sup>2</sup> and 2.5 GGy gamma dose, does not differ from  $I_{RL}$  of nonirradiated samples with the exception of the 600–700 nm region. A prompt transparency decrease of the quartz specimen during the neutron pulse is absent within the experimental error and does not influence the radioluminescence intensity measurements.
4. No difference was observed in the radioluminescence intensity for quartz samples irradiated at temperatures of 18°C and 100°C.
  5. Estimates for quartz windows have shown that  $I_{RL}$  is much lower than the bremsstrahlung intensity from thermonuclear reactor plasmas.
  6. The radioluminescence does not prevent the use of optical windows made from KU-1 fused quartz for the visible spectral range in thermonuclear reactor diagnostic systems.

#### Acknowledgements

This paper has been prepared as an account of work assigned to the RF Home Team under Task Agreement No. T-246 within the Agreement among the European Atomic Energy Community, the Government of Japan, the Government of the Russian Federation and the Government of the USA on Cooperation in the Engineering Design Activities for the International Thermonuclear Experimental Reactor (ITER EDA Agreement) under the auspices of the International Atomic Energy Agency (IAEA).

#### References

- [1] M.J. Treadway, B.C. Passenheim, B.D. Kittener, IEEE Trans. NS 22 (1975) 2253.
- [2] D.V. Orlinski, I.V. Altovsky, T.A. Basilevskaya, V.T. Gritsyna, V.I. In'kov, I.A. Ivanin, D. Kovalchuk, A.V. Krasilnikov, D.V. Pavlov, Yu.A. Tarabrin, S.I. Turchin, V.S. Voitsenya, I.L. Yudin, J. Nucl. Mater. 212 (1994) 1059.
- [3] A. Morono, E.R. Hodgson, J. Nucl. Mater. 224 (1995) 216.
- [4] T. Tanabe, S. Tanaka, K. Yamaguchi, N. Otsuki, T. Iida, M. Yamawaki, J. Nucl. Mater. 212 (1994) 1050.
- [5] A. Morono, E.R. Hodgson, J. Nucl. Mater. 258–263 (1998) 1889.
- [6] F. Sato, T. Iida, Y. Oyama, F. Maekawa, Y. Ikeda, J. Nucl. Mater. 258–263 (1998) 1897.
- [7] F. Sato, Y. Oyama, T. Iida, F. Maekawa, J. Datemichi, A. Takahashi, Y. Ikeda, Fusion Techn. (1996) 857.
- [8] D.V. Orlinski, K.Yu. Vukolov, Quartz KU-1 optical density measurements after irradiation in the nuclear reactor IR-8, Plasma Devices and Operations, in print.
- [9] V.I. In'kov, I.A. Ivanin, D.V. Orlinski, J. Nucl. Mater. 256 (1998) 254.
- [10] D.L. Griscom, K.M. Golant, A.L. Tomashuk, D.V. Pavlov, Yu.A. Tarabrin, Appl. Phys. Lett. 69 (1996) 322.
- [11] S.F. Paul, J.L. Golfstein, R.D. Durst, F.J. Fonck, Rev. Sci. Instrum. 66 (1995) 1252.
- [12] A.V. Krasilnikov, A.A. Ivanov, S.N. Tugarinov et al., Transmission and radioluminescence of all-silica optical fibres with Co60 gamma and reactor irradiations, Report on the Workshop on Diagnostic Components Radiation, St. Petersburg, 5 June 1997.
- [13] ITER EDA-JCT, 11 July 1995, S55 RE 1 95-07-11 F1.
- [14] V. Vershkov, V. Krupin et al., Russ. J. Plasma Phys. 10 (1984) 901.